Photoreaction of $[Ru(hat)_2phen]^{2+}$ with Guanosine-5′-Monophosphate and DNA: Formation of New Types of Photoadducts

Romain Blasius,[a] Hélène Nierengarten,[b] Michel Luhmer,[c] Jean-François Constant,[d] Eric Defrancq,[d] Pascal Dumy,[d] Alain van Dorsselaer,[b] Cécile Moucheron,[a] and Andrée Kirsch-DeMesmaeker*[a]

Abstract: $[Ru(hat)_2phen]^{2+}$ (HAT = 1,4,5,8,9,12-hexaazatriphenylene, phen = 1,10-phenanthroline) interacts with a good affinity with polynucleotides and DNA by intercalation, despite the presence of a second voluminous ancillary HAT ligand. It photoreacts with guanosine-5′-monophosphate (GMP). From HPLC, ESMS and NMR analyses, it can be concluded that this complex forms photoadducts with GMP. In contrast to the photoadducts isolated with Ru–TAP complexes (TAP = 1,4,5,8-tetraazaphenanthrene), the photoadducts with $[Ru(hat)_2phen]^{2+}$ contain a covalent link between the oxygen atom of the guanine unit and a HAT ligand. Formation of oxidised photoadducts and compounds resulting from the addition of two GMP entities to the complex are also detected as side products. In the presence of oligo- and polynucleotides, $[Ru(hat)_2phen]^{2+}$ yields photoadducts when guanine bases are present.

Keywords: DNA damage · guanosine · oxidation · photochemistry · ruthenium

Introduction

Transition-metal complexes have been extensively studied as probes of nucleic acids and metal-containing drugs during the last decade. Platinum complexes such as *cis*-$[PtCl_2(NH_3)_2]$ and derivatives are certainly the best examples of application of such compounds in chemotherapy.[1,2] The activity of these platinum drugs versus a variety of different types of cancer originates from their "dark" reaction with DNA, first by substitution of one or two chloride ligands by water molecules, followed by substitution by adjacent guanines in the DNA. Important toxic side effects of these drugs have motivated researchers to develop other metal-containing complexes. In this context, the interaction and photoreaction of Ru^{II} complexes with DNA have been the subject of intensive studies.[3–11] Some of these compounds turned out to be particularly attractive. In fact, they are able to produce, upon illumination, addition of the metal-containing complex to the guanine units of DNA, which inhibits certain enzymes such as RNA polymerase.[12] They could thus offer different advantages: i) their action would be triggered exclusively under illumination, a better control of the activity could thus be expected, ii) the type of their photoadducts is quite different from known metal-containing adducts; indeed contrary to the Pt complexes, their coordination sphere around the metal is kept unchanged after the photoadduct formation. The consequences at the level of the activity or effect of such photoadducts on the cellular function could thus be different and open the way to potential novel drugs.

We have shown in the past that the complexation of Ru^{II} to π-deficient ligands such as TAP (1,4,5,8-tetraazaphenan-

[a] Dr. R. Blasius,[+] Prof. C. Moucheron, Prof. A. Kirsch-DeMesmaeker
Université Libre de Bruxelles
Chimie Organique et Photochimie, CP 160/08
50 avenue F.D. Roosevelt, 1050 Brussels (Belgium)
Fax: (+32) 2-650-3018
E-mail: akirsch@ulb.ac.be

[b] Dr. H. Nierengarten, Prof. A. van Dorsselaer
Laboratoire de Spectrométrie de Masse Bio-organique
Faculté de Chimie, 1 rue Blaise Pascal
67008 Strasbourg (France)

[c] Prof. M. Luhmer
Université Libre de Bruxelles
RMN Haute Résolution, CP 160/08
50 avenue F. D. Roosevelt, 1050 Brussels (Belgium)

[d] Dr. J.-F. Constant, Dr. E. Defrancq, Prof. P. Dumy
LEDSS, UMR CNRS 5616
Université Joseph Fourier, BP 53
38041 Grenoble cedex 9 (France)

[+] Present address:
Laboratoire de Biologie Moléculaire et Cellulaire du Cancer
Hôpital Kirchberg
9 rue Edward Steichen, 2540 Luxembourg (Luxembourg)

Supporting information for this article is available on the WWW under http://www.chemeurj.org/ or from the author.

 DOI: 10.1002/chem.200400591

threne) led to complexes that, upon illumination oxidise the guanine units[13–15] by an electron transfer from the guanine base to the excited Ru complex.[4,13,15–17] The resulting ligand radical anion in the complex and guanine radical cation undergo an acid–base reaction with protonation of the complex and deprotonation of the guanine unit. The two radicals react and lead to formation of a photoadduct with a covalent link between these two species.[4,13,14,18–20] However, most of the TAP based photoreactive complexes studied until now exhibit a low affinity for polynucleotides and DNA.

An increased affinity for the polynucleotides can be achieved by using extended aromatic ligands such as the well known DPPZ (dipyrido[3,2-*a*;2′,3′-*c*]phenazine)[21–24] or the PHEHAT (1,10-phenanthrolino[5,6-*b*]1,4,5,8,9,12-hexaazatriphenylene)[25,26] ligand that intercalate into the stacking of bases. However, these ligands do not make the resulting complexes photoreactive.

In this work, we examine the behaviour of $[Ru(hat)_2phen]^{2+}$ (phen = 1,10-phenanthroline) (Figure 1) in the presence of mono- and polynucleotides. The goal is two-folded: i) to show whether a HAT ligand is capable of playing the role of a typical intercalating ligand such as dppz or PHEHAT and thus capable of favouring the interaction with DNA, and ii) to check and study the photoreactivity of $[Ru(hat)_2phen]^{2+}$ versus mono-, polynucleotides and nucleic acids.

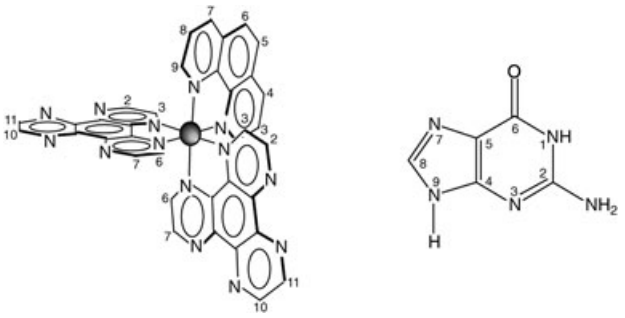

Figure 1. Structure of $[Ru(hat)_2phen]^{2+}$ (PHEN = 1,10-phenanthroline, HAT = 1,4,5,8,9,12-hexaazatriphenylene) and guanine for the numbering of the protons.

Results

Interaction with polynucleotides—Comparison with the TAP complexes: Figure 2 shows the dependence of the relative emission intensities I/I_0 of $[Ru(hat)_2phen]^{2+}$ as a function of the concentration of polynucleotide (in equivalents of phosphate) in buffered solution at pH 7 (10 mM Tris-HCl). The concentration of the complex (c_t) was kept constant. The relative emission intensity decreases in the presence of calf thymus (CT)-DNA till a plateau value of 0.18 (Figure 2, Table 1). This emission quenching originates from an electron transfer from the guanine bases of DNA to the excited complex.[15,16] At the highest DNA concentration, the luminescence quenching (I_∞/I_0) is comparable to that observed with $[Ru(tap)_3]^{2+}$[4,13] ($I_\infty/I_0 = 0.2$)[27] but is higher than for the TAP homologous complex $[Ru(tap)_2phen]^{2+}$ ($I_\infty/I_0 = 0.35$ under the same conditions)[28] which has approximately the same oxidizing power as $[Ru(hat)_2phen]^{2+}$. This indicates that the process of electron transfer is more efficient in $[Ru(hat)_2phen]^{2+}$ than in $[Ru(tap)_2phen]^{2+}$ despite the same redox properties. This could be due as demonstrated below to a better interaction of $[Ru(hat)_2phen]^{2+}$ with CT-DNA. The luminescence quenching contrasts the luminescence enhancement of $[Ru(hat)_2phen]^{2+}$ in the presence of $[poly(dA\text{-}dT)]_2$ up to a plateau value of 1.84 due to i) a protection of the luminophore by the polynucleotide from H_2O or O_2[29] and ii) the absence of quenching because $[Ru(hat)_2phen]^{2+}$ in the excited state cannot oxidise adenine or thymine units. A higher plateau value is reached in the case of $[Ru(hat)_2phen]^{2+}$ than for the TAP complexes[4,13,28] because of a better protection of excited $[Ru(hat)_2phen]^{2+}$ by the polynucleotide. The titration curves in Figure 2 reflect the shift of the binding equilibrium of $[Ru(hat)_2phen]^{2+}$ for DNA and $[poly(dA\text{-}dT)]_2$ with the polynucleotide concentration. The $([polynucleotide]/c_t)_{1/2}$ ratios correspond to 50% of the maximum variation of the emission; these values change inversely with the values of the association constants. Thus, the comparison of these $([polynucleotide]/c_t)_{1/2}$ ratios in Table 1 indicates the relative magnitudes of the binding constants.[30] The $([polynucleotide]/c_t)_{1/2}$ value is lower for $[Ru(hat)_2phen]^{2+}$ than for other Ru^{II} complexes whose affinity constants were determined previously by luminescence titration in the same conditions (Table 1), thus again in agreement with a better interaction of this complex with polynucleotides. Titrations by luminescence of $[Ru(hat)_2phen]^{2+}$ with CT-DNA were also investigated by emission lifetimes measurements. The ratios τ/τ_0 and I/I_0 as a function of the CT-DNA concentration (in phosphate equivalents) are compared in Figure 3. The difference between the two curves suggests that the emission quenching of $[Ru(hat)_2phen]^{2+}$ by the guanine bases of CT-DNA is not only dynamic, but there is also contribution of some static quenching. This latter can be calculated according to Equation (1):

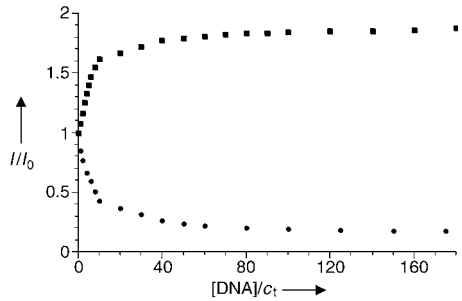

Figure 2. Emission titration of rac $[Ru(hat)_2phen]^{2+}$ with CT-DNA (●) and $[poly(dA\text{-}dT)]_2$ (■). All the experiments were performed in the presence of 10 mM Tris-HCl buffer, pH 7. The concentration of $[Ru(hat)_2phen]^{2+}$ (c_t) was kept constant at 5 μM while the polynucleotide concentration (expressed in phosphate concentration) was increased; I is the emission intensity in the presence of the polynucleotide and I_0 is the emission intensity in the absence of polynucleotide.

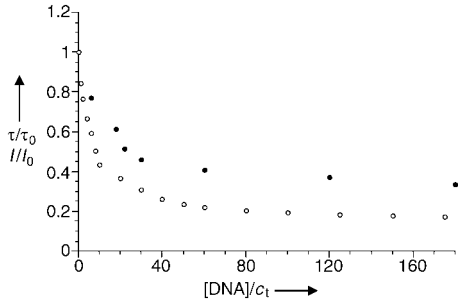

Figure 3. Relative emission intensity (○) and relative emission lifetime (●) for $[Ru(hat)_2phen]^{2+}$ titrated with CT-DNA. The experiments were performed in the presence of 10 mM Tris-HCl buffer, pH 7. The concentration of $[Ru(hat)_2phen]^{2+}$ (c_t) was kept constant at 5 μM while the DNA concentration (expressed in equivalents of phosphate concentration) was increased; $I(\tau)$ is the emission intensity (lifetime) in the presence of CT-DNA and $I_0(\tau_0)$ is the emission intensity (lifetime) in the absence of CT-DNA.

$$A_s = 1 - \frac{I/I_0}{\tau/\tau_0} \quad (1)$$

where A_s is the contribution of static quenching, I (or τ) the emission intensity (or lifetime) in the presence of CT-DNA and I_0 (or τ_0) the emission intensity (or lifetime) in the absence of CT-DNA. A 45% contribution of static quenching is calculated from Equation (1) for $[Ru(hat)_2phen]^{2+}$ with CT-DNA. This contribution is more important than the 15% static quenching previously determined for the non-intercalating complex $[Ru(tap)_2phen]^{2+}$,[31] which indicates again a better binding of the HAT than the TAP compound.

The binding equilibrium constants determined as described in the Experimental Section from the emission titration curves, are given in Tables 1 and 2. It may be concluded that $[Ru(hat)_2phen]^{2+}$ interacts less efficiently with polynucleotides than complexes containing a classical intercalating ligand such as a DPPZ or a PHEHAT ligand. However, $[Ru(hat)_2phen]^{2+}$ presents a much higher affinity for the polynucleotides than the TAP photoreactive ruthenium(II) complexes, which would originate from a better partial intercalation of one HAT ligand between the stacking of bases.

According to the data of reverse salt titrations with NaCl (see Experimental Section), the binding of $[Ru(hat)_2phen]^{2+}$ releases only 0.9 counterions, thus less than expected. Such low $Z\Psi$ values could be attributed to a coupled anion release upon Na^+ addition as suggested in the literature.[30,32] The salt effect analysis also allows the separation of the binding free energy ΔG^0 into two different contributions. These thermodynamic parameters are given in Table 2 and are compared to the values obtained for other Ru^{II} complexes. They show that the interaction is essentially controlled by non-electrostatic interactions, as it is the case for some intercalating complexes (Table 2), in contrast to non-intercalating compounds such as $[Ru(bpy)_2phen]^{2+}$.

Table 2. Comparison of thermodynamic parameters[a] corresponding to the binding of Ru^{II} complexes to DNA.

Complex	K_{obs}/ 10^4 M^{-1}	ΔG^0/ kJ mol^{-1}	$Z\Psi$	ΔG^0_{pe}/ kJ mol^{-1}	ΔG^0_{ne}/ kJ mol^{-1}
rac-$[Ru(hat)_2phen]^{2+}$	0.56	−21.1	0.9	−6.7	−14.4
rac-$[Ru(bpy)_2phen]^{2+}$ [30]	0.055	−15.6	1.6	−11.6	−4.0
Δ-$[Ru(phen)_3]^{2+}$ [32][b]	0.97	−22.6	1.4	−10.0	−13.0
Λ-$[Ru(phen)_3]^{2+}$ [32][b]	1.07	−23.0	1.2	−8.8	−14.2
rac-$[Ru(phen)_2dppz]^{2+}$ [21][b]	320	−37.2	1.9	−13.8	−23.4
ethidium [32][b]	49.4	−32.2	0.75	−5.0	−27.2

[a] K_{obs}: binding constant of the complex to DNA in solution containing 50 mM NaCl and 10 mM Tris-HCl buffer (pH 7) at 25 °C unless otherwise specified. ΔG^0: binding free energy. ΔG^0_{pe} and ΔG^0_{ne}: the polyelectrolyte and the non-electrostatic contributions to the binding free energy, respectively. The polyelectrolyte contribution for $[Na^+] = 50$ mM was calculated from $\Delta G^0_{pe} = Z\Psi RT \ln[M^+]$ whereas the non-electrostatic part of the free energy was calculated by difference, $\Delta G^0 = -RT\ln K_{obs} = \Delta G^0_{ne} + \Delta G^0_{pe}$. [b] Experiments performed in solution containing 50 mM NaCl and 5 mM Tris-HCl buffer (pH 7.1) at 20 °C.

This study of interaction of $[Ru(hat)_2phen]^{2+}$ with polynucleotides was completed by viscosity measurements. The viscosity data with CT-DNA[33] in the presence of $[Ru(hat)_2phen]^{2+}$ are compared in Figure 4 with those obtained for the known intercalators $[Pt(bpy)(py)_2]^{2+}$ and $[Pt(bpy)(en)]^{2+}$ (en = ethylenediamine) that are also doubly charged metal complexes.[34–37] The behaviours are similar, the increase of viscosity is, however, slightly lower with $[Ru(hat)_2phen]^{2+}$ than with ethidium bromide.[32]

In conclusion, all these data indicate intercalation of a HAT ligand of $[Ru(hat)_2phen]^{2+}$, at least partially, despite the presence of the second rather large HAT ligand.

Photoadduct formation with GMP: Photoadduct formation between a complex and mononucleotides can be monitored by UV/Vis absorption spectroscopy.[15,18,20,38] Steady state illuminations were carried out with the complex alone and in the presence of GMP. No change in the absorption spectra were observed after several hours of illumination of the complex alone; this suggests that $[Ru(hat)_2phen]^{2+}$ does not undergo photodechelation. By contrast,

Table 1. Relative plateau values (I_∞/I_0) from the titration curves with CT-DNA or $[poly(dA\text{-}dT)]_2$ and corresponding calculated binding constants (K_{obs}) in Tris-HCl buffer, for $[Ru(hat)_2phen]^{2+}$ and other reference compounds.

Compound	Polynucleotide	[NaCl] /mM	I_∞/I_0	([polynucleotide] $/c_t)_{1/2}$	$K_{obs}/10^4$ M^{-1}
rac-$[Ru(hat)_2phen]^{2+}$	CT-DNA	0	0.18	6	24
	$[poly(dA\text{-}dT)]_2$	0	1.84	5	38
rac-$[Ru(bpy)_2phen]^{2+}$ [30]	CT-DNA	0	1.84	21	0.84
rac-$[Ru(tap)_2phen]^{2+}$ [28,31]	CT-DNA	0	0.35	16	3.9
Λ-$[Ru(phen)_2dppz]^{2+}$ [21]	CT-DNA	50	–	–	170
Δ-$[Ru(phen)_2dppz]^{2+}$ [21]	CT-DNA	50	–	–	320

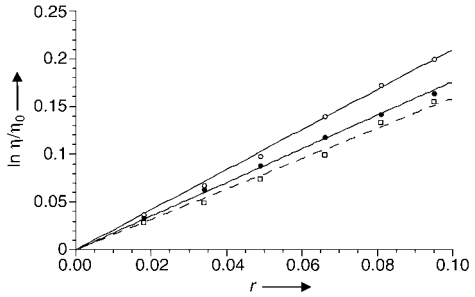

Figure 4. Titration of CT-DNA (6.0×10^{-4} M) with $[Ru(hat)_2phen]^{2+}$ by viscosity measurements (●) and the known intercalators $[Pt(bpy)(py)_2]^{2+}$ (○) and $[Pt(bpy)(en)]^{2+}$ (□), in 2 mM phosphate buffer and 9 mM NaCl. η = intrinsic viscosity of sonicated DNA in the presence of the complex. η_0 = intrinsic viscosity of sonicated DNA in the absence of the complex. r = [complex]/[DNA], [DNA] in phosphate equivalents.

changes of absorption were recorded as a function of visible irradiation of $[Ru(hat)_2phen]^{2+}$ (2×10^{-5} M) in the presence of GMP (2×10^{-2} M, 100 mM Tris-HCl pH 7). The results are shown in Figure 5 for solutions saturated with oxygen and argon. An increase of the absorption between 300 and 475 nm occurs in both cases and the enhancement is much more important around 300 nm for the oxygen than for the argon saturated solution. The evolution of the absorption spectra in an air-saturated solution was intermediate between the two other cases.

ES mass spectrometry analysis of the photoproducts formed in the presence of GMP: In order to explain the differences in the evolution of the absorption spectra under oxygen, air and argon, the products formed under illumination were analysed by electrospray mass spectrometry (ESMS). For these analyses, the photoproducts were first separated by HPLC. Figure 6 shows a typical chromatogram obtained after visible irradiation of $[Ru(hat)_2phen]^{2+}$ in the presence of GMP in argon saturated aqueous solution. The first peak (at 1 min) has the same retention time and absorption spectrum as GMP ($\lambda_{max}=272$ nm). The peak detected at 7.7 min in the chromatogram exhibits a bathochromic absorption ($\lambda_{max}=302$ nm) compared with the absorption of GMP. This might indicate the presence of oxidised GMP such as in 8-oxoguanosine monophosphate for example ($\lambda_{max}=292$ nm). All the peaks detected after 14 minutes correspond to metal-containing complexes because they exhibit a strong absorption in the visible region, typical of MLCT absorptions. The peak at 14–15 min is attributed to the starting complex $[Ru(hat)_2phen]^{2+}$, as indicated by the absorption and ES mass spectra (legend of Figure 6). The set of peaks detected between 18 and 25 min and collected together because no efficient separation could be obtained gave the ESMS data gathered in Table 3. Two species (*m*/*z* 555.5, 27% and *m*/*z* 1110.2, 8%) correspond to a photoadduct formed between $[Ru(hat)_2phen]^{2+}$ and i) a neutral GMP (thus A + C − 2H) or ii) a negatively charged GMP (thus A + D − 2H). A third species (*m*/*z* 449.7, 100%) corresponds to an adduct between $[Ru(hat)_2phen]^{2+}$ and a guanine (thus A + B − 2H). The loss of the sugar phosphate could stem from decomposition in ESMS analysis. Indeed, when GMP alone was analysed directly by ES mass spectrometry, the sugar and phosphate residues were also partially lost. Finally in the set of peaks at 18–25 min (Table 3), another species was detected at *m*/*z* 736.5. This peak fits with the mass of a biadduct, that is, the addition of two uncharged GMP nucleotides on one $[Ru(hat)_2phen]^{2+}$ (thus A + 2C − 4H). As this peak corresponds to a secondary photoproduct, we did not succeed to obtain enough material (even for longer illumination times, see below) to determine the structure of the biadduct or to gather arguments in favour of the addition of the two GMP entities to the same ligand or to two different ligands. The absorption spectra of the five HPLC peaks at 18–25 min were quite similar and exhibited a hypsochromic shift of 17 nm compared with the starting complex (from 410 nm for the

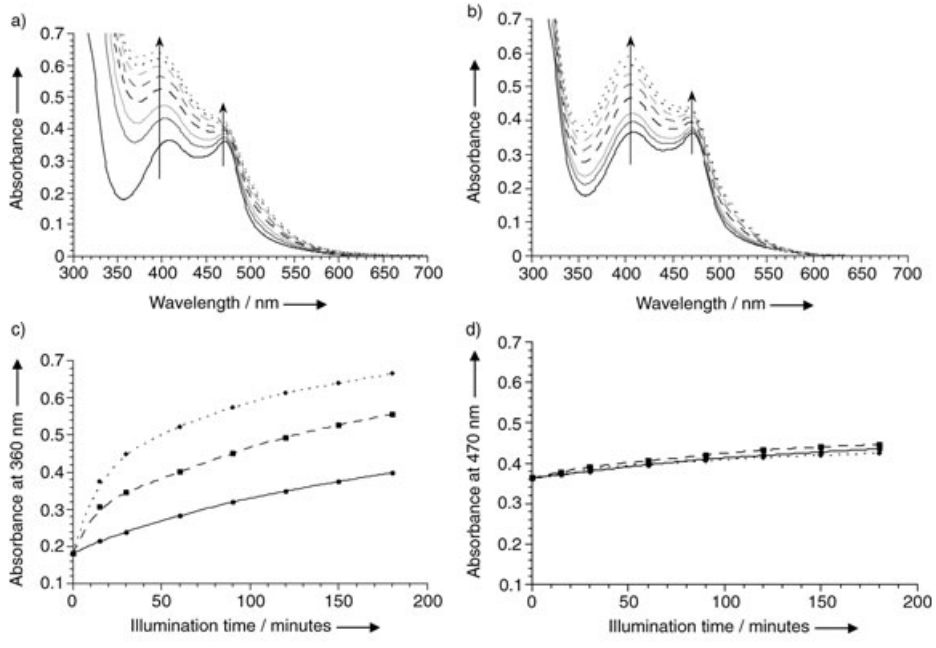

Figure 5. a) and b): Changes in the absorption spectra of $[Ru(hat)_2phen]^{2+}$ ($2\ 10^{-5}$ M) under visible irradiation in the presence of GMP ($2\ 10^{-2}$ M) at pH 7. a) oxygen-saturated solution. b) Argon-saturated solution; t = 0, 15, 30, 60, 90, 120, 150, 180 min. c) and d) Evolution of the absorption of $[Ru(hat)_2phen]^{2+}$ under visible irradiation in the presence of GMP as a function of time under argon (●), air (■) and oxygen (◆); c) at 360 nm; d) at 470 nm.

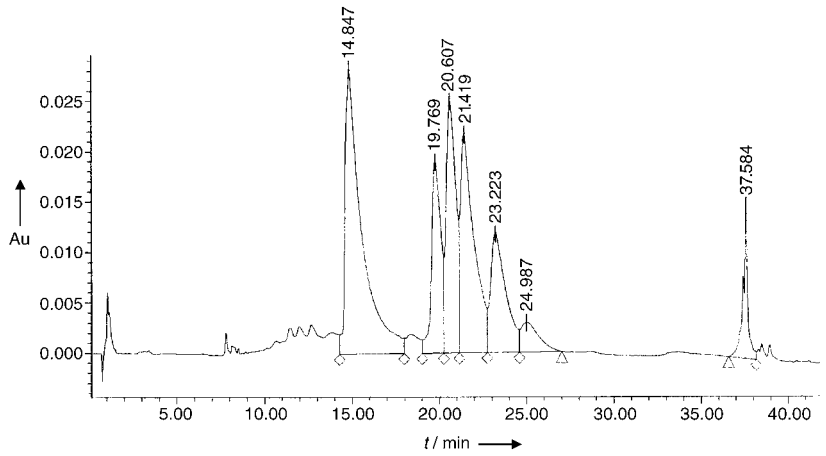

Figure 6. Chromatogram of the solution after 3 h of irradiation of $[Ru(hat)_2phen]^{2+}$ in the presence of GMP under argon. The detection was performed by absorption at 410 nm. ES mass spectrometry data: Peak at 14–15 min, $[Ru(hat)_2phen]^{2+}$ ($[M-2Cl^-]^{2+}$ calculated *m/z* 374.9; found *m/z* 375.2; relative intensity 100% and $[M-2Cl^-+CF_3COO^-]^+$ calculated *m/z* 862.7; found *m/z* 863.2; relative intensity 25%), the set of peaks between 18 and 25 min, see Table 3 and at 37 min, see Table 4.

Table 3. Mass spectra of the products between 18 and 25 min.

m/z	Calculated *m/z*	Intensity (%)	Charge	Product[a]
449.7	449.4	100	2+	A + B − 2H
555.5	555.5	27	2+	A + C − 2H
736.5	736.1	12	2+	A + 2 C − 4H
1110.2	1109.9	8	1+	A + D − 2H

[a] A = complex (cf. Figure 1), B = guanine, C = GMP with the phosphate under the form $H_2PO_4^-$, and D = GMP with the phosphate under the form HPO_4^{2-}; −2H = formation of the covalent bond between the ruthenium(II) complex and the base with loss of two hydrogen atoms.[13,14,18–20] Illumination time: 3 h.

Table 5. Mass data for the products between 18 and 25 min after longer illumination times ($t = 10$ h).

m/z	Calculated *m/z*	Intensity (%)	Charge	Product[a]
449.5	449.4	82	2+	A + B − 2H
524.2	524.0	22	2+	A + 2 B − 4H
555.5	555.5	28	2+	A + C − 2H
630.0	630.0	57	2+	A + B + C − 4H
736.5	736.1	100	2+	A + 2 C − 4H

[a] A, B, C and D, as defined in Table 3.

starting complex, to 393 nm). Such shifts were observed previously for photoadducts between polyazaaromatic Ru^{II} complexes and GMP.[15,20,38] The ESMS data for the products around 37 min are given in Table 4. The predominant peak (*m/z* 457.7) would correspond to a photoadduct of $[Ru(hat)_2phen]^{2+}$ with one oxidised guanine residue, and the two other peaks (*m/z* 563.8 and 1126.2) to similar photoadducts that have kept their phosphate (non-ionised and ionised, respectively). The absorption spectra of the corresponding HPLC peaks (at 37 min) also present a hypsochromic shift of the MLCT band from 410 to 382 nm as compared to the starting $[Ru(hat)_2phen]^{2+}$.

Table 4. Mass data for the products eluted after 37 min.

m/z	Calculated *m/z*	Intensity (%)	Charge	Product[a]
457.7	457.4	100	2+	A + B + O − 2H
563.8	563.5	28	2+	A + C + O − 2H
1126.2	1125.9	20	1+	A + D + O − 2H

[a] A, B, C and D, as defined in Table 3. O = oxygen atom.

Experiments for longer illumination times of $[Ru(hat)_2phen]^{2+}$ in the presence of GMP were also carried out. Under these conditions, the relative amount of products that could correspond to biadducts increased (Table 5). Among them, masses that fit with the addition of two guanines, or two guanidines or one guanine plus one guanidine, could be found. Isotopic distributions of all the peaks corresponding to the masses of the mono- and biadducts are in agreement with the calculated distribution (see Supporting Information).

It was also observed that the amount of photoadduct formed under illumination (3 h) depends strongly on the oxygen concentration in solution. Unreacted $[Ru(hat)_2phen]^{2+}$ decreases with increasing oxygen concentration and the peaks at 7.7 and 37 min increase in agreement with their attribution to oxidised GMP and oxidised photoadducts, respectively. Moreover the total amount of photoadduct increases with higher oxygen concentrations contrary to what was expected.

Characterisation of the photoadduct(s): In order to gain information on the structure of the photoadduct(s) (corresponding to the HPLC peaks at 18–25 min), the photoreaction under argon was scaled up to produce larger amounts of the target compounds. The photoadducts formed in such a photolysed solution were isolated by cation-exchange chromatography followed by a further separation by HPLC. Since the sample isolated in this way did not contain biadduct as shown by ESMS, this sample was characterised by ^1H NMR spectroscopy in D_2O and in $[D_6]DMSO$. The chemical shifts for the photoadduct(s) in D_2O are gathered in Table 6 (for ^1H NMR spectrum and DQF-COSY spectrum see Supporting Information). The formation of photoadduct between the $[Ru(hat)_2phen]^{2+}$ and another moiety such as GMP should result in

Table 6. NMR data in D_2O. Chemical shifts of the aromatic protons of the photoadducts. H_X^H refers to the protons on a HAT ligand, H_X^P refers to the protons on the phen ligand and G_8 refers to proton 8 of the guanosine-5′-monophosphate.

	$[Ru(hat)_2phen]^{2+}$			Adduct A (30%)		Adduct B (70%)	
Proton	δ	Int.	Proton	δ	Int.	δ	Int.
$H^H_{10,11}$	9.47	4 H	$H^H_{10,11\alpha}$	9.51 and 9.43	2 H	9.51 and 9.43	2H
			$H^H_{10,11\beta}$	9.48	2H	9.47	2H
H^H_7	9.20	2H	$H^H_{7\alpha}$			9.03	1H
			$H^H_{7\beta}$	9.13	1H	9.20	1H
H^H_2	9.15	2H	$H^H_{2\alpha}$	9.06	1H		
			$H^H_{2\beta}$	9.24	1H	9.22	1H
H^H_6	8.70	2H	$H^H_{6\alpha}$	8.45	1H	8.32	1H
			$H^H_{6\beta}$	8.44	1H	8.28	1H
H^H_3	8.49	2H	$H^H_{3\alpha}$	8.52	1H	8.41	1H
			$H^H_{3\beta}$	8.90	1H	8.74	1H
$H^P_{4,7}$	8.81	2H	$H^P_{4,7}$	8.80	2H	8.80	2H
$H^P_{5,6}$	8.36	2H	$H^P_{5,6}$	8.34	2H	8.34	2H
$H^P_{2,9}$	8.27	2H	H^P_9	8.26	1H	8.22	1H
			H^P_2	8.22	1H	8.45	1H
$H^P_{3,8}$	7.81	2H	$H^P_{3,8}$	7.81	2H	7.81	2H
G_8			G_8	8.46	1H	8.46	1H

the loss of the C_2 symmetry of the complex and induce a differentiation of most of the protons. This is clearly observed in the NMR spectrum. Furthermore, the signals 2 and 7 of the HAT ligand (Figure 1 for the numbering) do not integrate to four protons as in the spectrum of $[Ru(hat)_2phen]^{2+}$, but for three protons, which indicates the loss of one proton due to the photoadduct formation. The integrations of the other protons on the HAT and phen ligands are the same as in the starting $[Ru(hat)_2phen]^{2+}$. Consequently the photoadduct is clearly formed on the positions 2 and 7 of the HAT ligand. Furthermore, two systems corresponding to two geometric isomers can be identified with a DQF-COSY spectrum. Integration indicates an excess (70:30) of isomer B (covalent bond in the photoadduct at position 2 of the HAT ligand) over isomer A (covalent bond in the photoadduct at position 7 of the HAT ligand) (Figure 7).

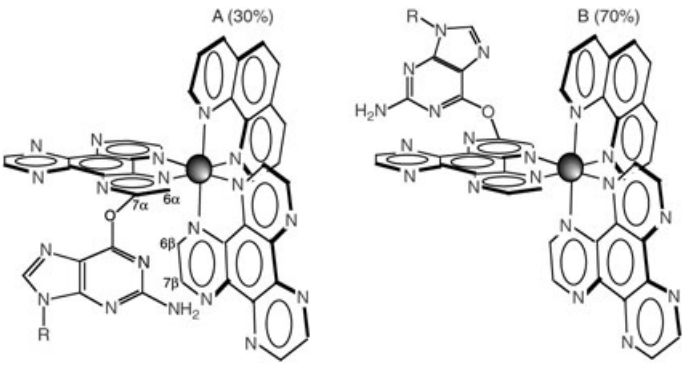

Figure 7. Structures proposed for the two photoadduct isomers between $[Ru(hat)_2phen]^{2+}$ and GMP. R represents the sugar-phosphate group of the GMP moiety.

In order to gain information on the position of the covalent bond on the guanine moiety, we performed NMR measurements with the photoadduct in $[D_6]$DMSO, which prevents the exchange of the heteroatomic protons. In this spectrum, we could observe the presence of two protons on the exocyclic nitrogen with the disappearance of proton number 1 of the guanine moiety (see Figure 1 for the numbering of the guanine protons). This leads us to the conclusion that the guanine moiety is linked to the HAT ligand via the nitrogen 1 or the exocyclic oxygen (enol tautomer). On the other hand, the NMR data also show that the photoadduct should contain the sugar phosphate moiety (signals from 4.1 to 5.9 ppm in the DQF-COSY spectrum).

In conclusion, the NMR analyses indicate that two photoadduct isomers (A and B, Figure 7) are formed. Moreover as the sugar moiety is chiral and as the metal centre can be Δ or Λ, two diastereosiomers can exist for each isomer A and B. The four HPLC peaks at 18–25 min could thus correspond to these four compounds.

The photoadduct analysed by NMR spectroscopy was also characterised by absorption spectroscopy and steady-state and time-resolved emission. The band between 370 and 420 nm (Figure 8) exhibits a hypso- and hyperchromic effect when the absorption of the sample and that of $[Ru(hat)_2phen]^{2+}$ is adjusted to the same absorption at 460 nm. The emission of the photoadduct is extremely weak compared with that of $[Ru(hat)_2phen]^{2+}$; indeed if we assume that the absorption coefficients are on the same order of magnitude at 460 nm (thus when the absorbance is adjusted at the same value at this wavelength), the photoadduct emits at the same λ_{max} (650 nm) but ~250 times less than $[Ru(hat)_2phen]^{2+}$ and with an emission lifetime of ~5 ns, thus much shorter than the emission lifetime of $[Ru(hat)_2phen]^{2+}$ (640 ns).

Photoadduct formation with CT-DNA and oligonucleotides: Steady state illuminations of $[Ru(hat)_2phen]^{2+}$ were also carried out in the presence of CT-DNA under argon, air and oxygen. Figure 9 shows the changes of the absorption spec-

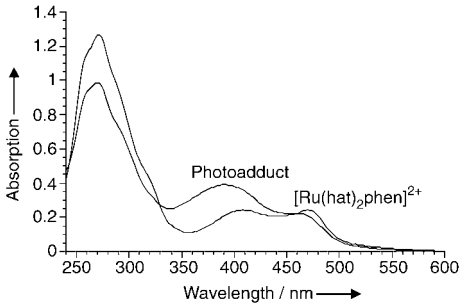

Figure 8. Absorption spectra of the photoadduct and $[Ru(hat)_2phen]^{2+}$ in water. The absorption was adjusted to the same value for the two compounds in their MLCT band at 460 nm.

tra as a function of the illumination time for a ratio CT-DNA (in nucleotides equivalents) over complex concentration of 100 ($[Ru(hat)_2phen]^{2+} = 2\times10^{-5}$ M; $[DNA] = 2\times10^{-3}$ M). An increase of the absorption appeared around 400 nm; however, no oxygen effect was detectable (Figure 9a and b). These absorption changes are similar to those observed with GMP (except the absence of oxygen effect) and would thus correspond to the formation of photoadducts on the guanine residues of CT-DNA. In order to confirm this, illumination experiments were performed with oligodeoxyribonucleotides.

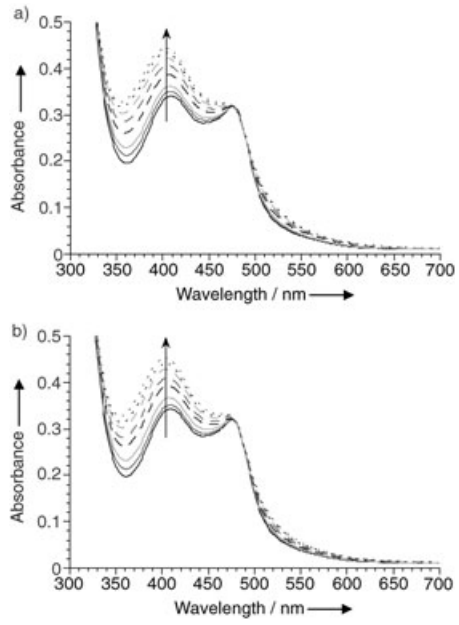

Figure 9. Changes in the absorption spectra of $[Ru(hat)_2phen]^{2+}$ (2×10^{-5} M) under visible irradiation in the presence of CT-DNA (2×10^{-3} M) at pH 7. a) Air-saturated solution. b) Argon-saturated solution. Irradiation: t = 0, 15, 30, 60, 90, 120, 150, 180 min.

Denaturing gel electrophoresis experiments with 17-mer oligodeoxyribonucleotides: The formation of photoadducts with synthetic oligonucleotides was monitored by gel electrophoresis in denaturing conditions. Three different double stranded oligonucleotides containing guanines in different sequences (Figure 10) were illuminated with visible light (above 350 nm) in the presence of $[Ru(hat)_2phen]^{2+}$ and in the presence of $[Ru(tap)_2phen]^{2+}$ as a standard. Duplex sequence 0, which does not contain any guanine residue was used as a blank. Figure 11 shows the electrophoregram obtained for a typical illumination experiment of duplex sequence 3 (10^{-6} M) in the presence of $[Ru(hat)_2phen]^{2+}$ (2×10^{-5} M) in aerated buffered solution (Tris-HCl, 5 mM, pH 7). Lane A corresponds to the non-illuminated sample and lane B to the same sample after 30 min illumination, in both cases in the absence of $[Ru(hat)_2phen]^{2+}$. In lane C, the duplex was illuminated for 30 min in the presence of $[Ru(hat)_2phen]^{2+}$. One can observe the appearance of a less mobile species corresponding to the photoaddition of ruthenium complex on the oligonucleotide. Illumination experiments performed with the oligonucleotide duplex 0 (which does not contain guanines) did not lead to the occurrence of a slower migrating band. The occurence of frank breaks during illumination was not detected as illustrated by the absence of bands of higher mobility.

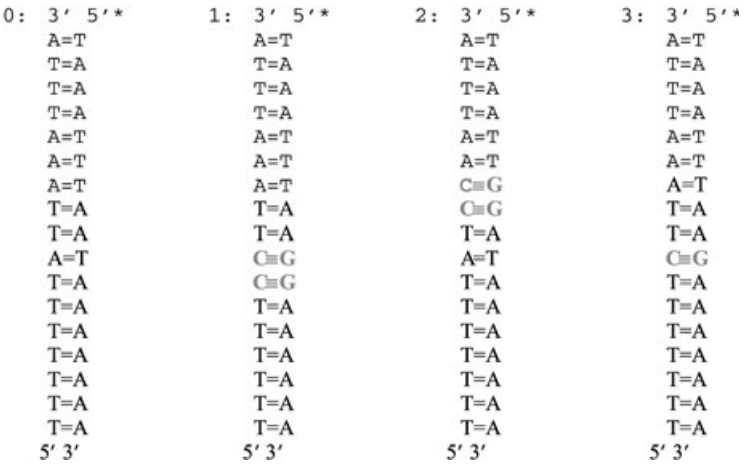

Figure 10. The different sequences of oligodeoxyribonucleotide duplexes for the gel electrophoresis experiments.

The formation of guanine oxidation products was investigated by chemical treatment (using hot piperidine) or enzymatic treatment (using fpg or formamido pyrimidine glycosylase) on oligonucleotides isolated from the gel after their illumination with the complex. Both treatments are known to cleave DNA at oxidised guanine positions (Fpg is specific for 8-oxo deoxyguanosine and other products of guanine oxidation) and would produce shorter fragments of higher mobility on an electrophoresis gel.[39–46] For this purpose, the slower migrating band (called "photoadducts") and the band which migrates as the starting material ("17 mers" which might contain non modified strand and/or strand containing guanine oxidation products) were isolated from the gel and treated with piperidine or Fpg. Lane D and G correspond to the "17 mers" and the "photoadducts", respectively, before the treatment. Piperidine treatment (lane E), as

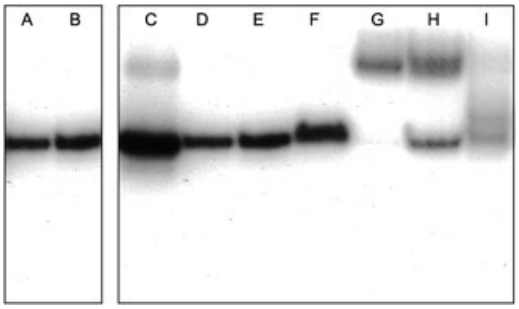

Figure 11. Photoadduct formation between $[Ru(hat)_2phen]^{2+}$ and double stranded oligonucleotide sequence 3 (^{32}P-5′-end-labeled at the guanine containing strand) analysed by denaturing gel electrophoresis. Lane A: non-illuminated duplex. Lane B: duplex illuminated for 30 min in the absence of $[Ru(hat)_2phen]^{2+}$. Lane C: duplex illuminated in the presence of $[Ru(hat)_2phen]^{2+}$. Lane D: product isolated by purifying the fastest band from lane C. Lane E: same as D but after piperidine treatment at 90 °C for 1 hour. Lane F: product isolated by purifying the fastest band from lane C and after Fpg treatment. Lane G: product isolated by purifying the slowest band from lane C. Lane H: same as G but after piperidine treatment. Lane I same as G but after exonuclease III treatment.

well as Fpg treatment (lane F) of the "17 mers" did not induce strand cleavage. In the case of the isolated slower migrating band, piperidine treatment (lane H) produced a species migrating as the starting oligonucleotide but no cleavage products. The Fpg treatment had no effect. These results strongly suggest that the illumination in the presence of the Ru complex did not produce oxidised guanine residues.

The slower migrating oligonucleotide (attributed to photoadduct formed with guanine) was also treated with exonuclease III (lane I). This enzyme is responsible for 80% of the repair of abasic sites in *Escherichia coli* and has a strong 3′ exonuclease activity (it digests an oligonucleotide into mononucleotides, starting from its 3′ end[44,47]). The exonuclease III treatment (lane I) induced the quasi total transformation of the retarded products into a faster and smeary band. Nevertheless, this "faster" species migrated more slowly than the starting 17 mer oligonucleotide.

The results obtained with the other sequences (sequences 1 and 2), as well as with $[Ru(tap)_2phen]^{2+}$, were qualitatively similar to those described above with $[Ru(hat)_2phen]^{2+}$ and sequence 3.

Discussion

The photoadduct in Figure 7 could be formed in the following way. Previous studies have shown that the electron transfer from the guanine unit to the excited complex[4,13,15–17] is followed by the protonation of the reduced ligand. Actually the transferred electron would be located essentially on the nitrogen atoms in *para* position of the chelated nitrogens, where protonation would occur. Afterwards, the thus formed radical on a carbon atom in β position of the chelating nitrogens would react with the guanine radical. This would lead to the structure of the photoadduct of Figure 7 after re-aromatisation of the HAT. Furthermore, the excess of isomer B compared with A would be explained by more sterical hindrances in A, induced by the second HAT ligand as compared to the phen ligand. Moreover, in the NMR spectra in [D$_6$]DMSO, proton 1 of the guanine moiety has disappeared whereas the two protons on the exocyclic nitrogen are still present. Therefore, we suggest that the covalent bond would be formed via the oxygen atom of the guanine moiety. Indeed, it has been shown that the guanine radical cation deprotonates on nitrogen 1[48–50] and leads to a radical mainly located on the oxygen atom of the guanine.[51–55] Figure 7 shows the two resulting putative structures of the photoadducts in agreement with all the above-mentioned data.

The difference in the absorption spectra of the starting complex $[Ru(hat)_2phen]^{2+}$ and photoadduct (Figure 8) can be explained by the effect of substitution by the guanine moiety. The guanine unit attached via the oxygen atom plays the role of an electron donor group which should destabilise mainly the ligand centred π* orbitals of the so-modified HAT ligand and, to a lesser extent, the metal centred dπ orbitals. Therefore the dπ–π* transition from the Ru toward the HAT–GMP ligand, should shift hypsochromically as observed experimentally. By contrast, the emission maximum does not shift compared with that of the starting complex because the weak remaining emission originates from the lowest excited triplet state, that is, the ^{3}MLCT (metal-to-ligand charge transfer) of the Ru-nonmodified HAT. The weak emission and shortening of the luminescence lifetime of the photoadduct could stem from an intramolecular electron transfer from the attached GMP moiety to the metal-containing species in the excited state.

When the illumination of the complex with GMP is performed in the presence of oxygen, the ESMS analyses suggest also the appearance of a minor photoproduct that is, a photoadduct between $[Ru(hat)_2phen]^{2+}$ and an oxidised guanine moiety. Notably such oxidised species are produced only with GMP and not with polynucleotides. Several mechanisms discussed in the literature can explain the formation of such oxidised guanine bases: i) appearance of singlet oxygen, produced by photosensitization[39,40,51,56–62] ii) formation of $OH^{\bullet}$ or $O_2^{\bullet-}$ radicals that could originate from the reaction of the transient monoreduced ruthenium complex with O_2[4,15,17,25,40,42,52,61,63,64] iii) formation of the radical cation $GMP^{\bullet+}$ [40,48,51] Furthermore, since the transformation of $GMP^{\bullet+}$ into 8-oxoguanine does not necessarily require the presence of oxygen in solution,[40,48,51] the detection of some oxidised guanine units in the photoadducts during illuminations under argon is thus not surprising.

The results show also that with increasing oxygen concentrations in solution, $[Ru(hat)_2phen]^{2+}$ disappears more rapidly. This might be explained by the fact that oxidised guanine units such as for example 8-oxoguanine moieties are better reductants (0.53 eV vs NHE) than guanine moieties (0.85 eV vs NHE).[40] Consequently, the formation under illumination and in the presence of oxygen, of a better electron donor than GMP, increases the efficiency of the reac-

tion with time and explains the faster disappearance of the starting complex and faster appearance of photoproducts.

In the presence of CT-DNA, the spectroscopic data as a function of the illumination time show also the appearance of photoadducts but interestingly, no oxygen effect could be detected in this case. This would suggest that maybe no oxidised guanine units is formed during visible irradiation due to a reduced access of O_2 or water to the three transient species formed in the CT-DNA (three different species may be considered as possible source of production of oxidized guanine via the above-mentioned mechanisms: the excited and reduced metal complex and the guanine radical cation). Actually the results of the gel electrophoresis experiments performed with $[Ru(hat)_2phen]^{2+}$ in the presence of synthetic oligodeoxyribonucleotides are in agreement with this hypothesis (see below).

By gel electrophoresis in denaturing conditions, the photoadducts formation with the guanine residues in 17 mer oligonucleotides is evidenced by the detection of species with a lower mobility. By contrast, oligonucleotides containing no guanine (sequence 0) did not give rise to the formation of this retarded band. Illumination in the absence of $[Ru(hat)_2phen]^{2+}$ and incubation in presence of the metal-containing complex in the dark did not produce retarded bands confirming that the covalent binding of the metal complex to the oligonucleotide was due to light treatment. The absence of faster migrating bands on the gel indicates the absence of frank breaks as it has been reported for other Ru^{II} complexes.[6,40,65]

Treatment of the oligonucleotide isolated from the gel after illumination, by piperidine or Fpg enzyme, did not induce the formation of faster migrating species. This strongly suggests that oxidised guanine moieties were not produced. This result is in agreement with the conclusion drawn from the absorption experiments. The piperidine treatment of the slow migrating oligonucleotide isolated from the gel (attributed to photoadduct) (see lane H in Figure 11) transformed partly this species into another species migrating as the starting oligonucleotide. This could be due to a partial dechelation of the photoanchored $[Ru(hat)_2phen]^{2+}$. The loss of a $[Ru(hat)(phen)]^{2+}$ species leads to an oligonucleotide with the second HAT ligand remaining bound to a guanine residue. This modification does not introduce a change of charge and the slight increase in mass is not expected to induce a dramatic change in mobility. This dechelation of the ruthenium complex was also evidenced on the free $[Ru(hat)_2phen]^{2+}$ for which a similar piperidine treatment induced a loss of emission, a decrease in intensity of the metal-to-ligand charge transfer band in the absorption spectrum and the appearance of a new bathochromic absorption band characteristic of a bis-chelated complex. The treatment of the purified photoadduct with the repair enzyme exonuclease III showed that the action of this enzyme is inhibited, at least partially, by the presence of the photoadduct. The reaction products migrated faster than the photoadducts but more slowly than a 17 mer suggesting that the 3′ to 5′ exonuclease activity removes only a few nucleotides. The mass increase and the positive charges brought by the Ru^{II} complex retards the shortened oligonucleotide and makes it to migrate more slowly than the 17 mer starting material.

Conclusion

The results of this work show that $[Ru(hat)_2phen]^{2+}$ presents a much stronger interaction with CT-DNA and polynucleotides than the previously studied photoreactive non-intercalating ruthenium(II)–TAP complexes. The different results suggest that this affinity enhancement is due to a partial intercalation of one of the HAT ligands between the stacking of bases of CT-DNA or polynucleotides.

$[Ru(hat)_2phen]^{2+}$ photoreacts with GMP and leads to the formation of two photoadducts, geometrical isomers between $[Ru(hat)_2phen]^{2+}$ and one guanine unit. It is obvious that the photoadducts with $[Ru(hat)_2phen]^{2+}$ represent a type of adducts quite different from the dark adducts formed with Pt complexes and mononucleotides or DNA since contrary to the Pt compounds, the chelation sphere is not lost in the Ru^{II} photoadducts.

Different minor photoproducts were also detected: photoadducts between $[Ru(hat)_2phen]^{2+}$ and one oxidised guanine unit (depending on the conditions), and biadducts between the complex and two guanine units. This is the first time that such biadducts are observed. Photoadducts formation occurred also during the illumination of $[Ru(hat)_2phen]^{2+}$ with CT-DNA or synthetic oligonucleotides containing guanine bases. However, in that case no indication of oxidised guanine units was found.

Experimental Section

Materials: The synthesis and characterisation of $[Ru(hat)_2phen]^{2+}$ and $[Ru(tap)_2phen]^{2+}$ were performed as previously described.[15] The concentrations of the metal-containing complexes were determined optically using the absorption coefficient value ε given in the literature.[15] The Tris-HCl buffer (pH 7) stock standard solution was purchased from Sigma and the water was purified with a Millipore Milli-Q system. Calf thymus DNA (CT-DNA) and $[poly(dA\text{-}dT)]_2$ were purchased from Pharmacia. CT-DNA was dialysed exhaustively against a phosphate buffer solution and subsequently against water. The CT-DNA and $[poly(dA\text{-}dT)]_2$ concentrations are expressed in base pairs (bp) and were determined spectrophotometrically (CT-DNA: $\varepsilon_{260}=6600\,M^{-1}\,cm^{-1}$ per phosphate; $[poly(dA\text{-}dT)]_2$: $\varepsilon_{262}=6600\,M^{-1}\,cm^{-1}$ per phosphate).

The oligonucleotides (sequences 0, 1, 2, 3) were prepared by automated DNA synthesis on an Expedite DNA synthesiser (Perkin–Elmer) using standard β-cyanoethylphosphoramidite chemistry on a 1 μM scale. The oligonucleotides were purified by PAGE (polyacrylamide gel electrophoresis) by using TBE buffer and urea (7 M).

Instrumentation: The absorption spectra were recorded on a Perkin–Elmer Lambda UV/Vis spectrophotometer. The emission spectra were obtained with a Shimadzu RF-5001 PC spectrofluorimeter equipped with a xenon lamp (250 W) as exciting source and a Hamamatsu R-928 red sensitive photomultiplier tube for detection. The spectra were corrected for the instrument response. The luminescence lifetimes were measured by time-resolved single-photon counting (SPC) with an Edinburgh Instruments (Edinburgh, UK) FL-900 spectrometer, equipped with an N_2-filled discharge lamp (with a gas pressure of 0.4 bar, a 1.3 mm gap and 5.6 kV

between the electrodes) and a Peltier-cooled Hamamatsu R-995 photomultiplier tube. The emission decays were analysed with the Edinburgh Instruments software (version 3.00), based on non-linear least-squares regressions using a modified Marquardt algorithm. Excitation at 379 nm was used and the emission was measured at 646 nm, which corresponds to the emission maximum of $[Ru(hat)_2phen]^{2+}$.

The photoadduct was characterised by NMR and ESMS analyses. The NMR spectra were recorded in D_2O and in $[D_6]$DMSO with a 600 MHz Varian spectrometer. Electrospray mass spectra were obtained with an ES triple quadrupole mass spectrometer Quattro II (Micromass, Altrincham, UK) in the laboratory of Professor A. van Dorsselaer, at the University Louis Pasteur (Strasbourg, France).

Viscosity measurements were performed on a Cannon-Ubbelhode semi-microdilution viscosimeter (Series No 75, Cannon Instrument Co.) at the University of Messina (Messina, Italy). The viscosimeter contained 2 mL of sonicated CT-DNA solution (600 base pairs).

Analytical HPLC was performed on a Waters 600 controller with a Waters 600 pump and 996 Photodiode Array Detector, using an analytical Nova-Pak C_{18} (3.9×150 mm) column. The separation of the photoproducts was carried out by HPLC.

Binding equilibrium

Polynucleotide titrations: The binding constants of $[Ru(hat)_2phen]^{2+}$ to DNA were determined from luminescence titrations at fixed concentrations of complex (5 μM) with increasing concentrations of polynucleotides. The samples were excited at 408 nm, and the emission intensities were measured at 646 nm and corrected for the instrument response. The ruthenium/polynucleotide solutions were continuously stirred and allowed to equilibrate for 10 min before each measurement. All measurements were performed under air-saturated conditions.

Binding equilibrium constants and associated thermodynamic parameters: Quantitative treatment of the titration data allows the determination of the affinity constants.[66,67] Like for other complexes, we chose the McGhee and von Hippel model[66] which describes random non-cooperative binding to a lattice [Eq. (2)]:

$$\frac{\nu}{c_f} = K_{obs}\frac{(1-n\nu)^n}{[1-(n-1)\nu]^{n-1}} \quad (2)$$

ν is the binding ratio c_b/[polynucleotide] (c_b is the concentration of bound complex, [polynucleotide] is the concentration of the polynucleotide expressed in base pairs, bp), K_{obs} is the apparent binding constant for the experimental conditions (10 mM Tris-HCl buffer, pH 7, with or without 50 mM NaCl, Tables 1 and 2), n is the average size of the binding site expressed in number of base pairs, and c_f is the concentration of free complex. For the treatment of the data, the concentrations of bound (c_b) and free (c_f) complex for each concentration of DNA have to be determined. A mathematical approximation,[30] was used to calculate these concentrations. The advantage of this mathematical procedure is the fact that the I_∞/I_0 value can be retrieved from the curves where a plateau is not yet reached (which was the case for the titrations in the presence of 50 mM NaCl). For the calculation, the binding site size was fixed to 3 bp.

Salt dependence: Samples of ruthenium–DNA in Tris-HCl buffer (10 mM, pH 7) were used to perform reverse salt titrations with NaCl. The concentration of $[Ru(hat)_2phen]^{2+}$ was fixed to 5 μM with [DNA]/[Ru] ratios of 75. The results were treated as previously described[21,30,32,68,69] in order to determine the thermodynamic parameters of the binding and compare the binding free energies with the values reported for other complexes. These reverse titrations yielded the concentration of bound complex at each salt concentration $[M^+]$ and the corresponding calculated K_{obs}. Equation (3) is obtained from the polyelectrolyte theory of Record:[68,69]

$$\delta\log K_{obs}/\delta\log[M^+] = -Z\Psi \quad (3)$$

where Z is the charge of the metal-containing complex and Ψ is the fraction of counterions associated with each DNA phosphate ($\Psi=0.88$ for double-stranded B-form DNA).[68] Thus $Z\Psi=1.76$ for complexes bearing a 2+ charge (number of Na^+ counterions released upon binding).

Gel electrophoresis: The guanine containing oligonucleotides were 5′-end-labeled by T4 polynucleotide kinase using [γ^{32}P]-ATP 3000 Ci mmol^{-1} (Perkin Elmer Life Sciences) at 37 °C for 30 min. Double stranded target DNA was prepared by heating the radioactively labeled oligonucleotides with their complementary strand to 90 °C for 5 min and then annealing by slow cooling (1 h) to RT. A solution of $[Ru(hat)_2phen]^{2+}$ (2×10^{-5} M) in 5 mM Tris-HCl buffer (pH 7) and ^{32}P-labeled duplex oligonucleotide (10^{-6} M) was illuminated for 30 min at 4 °C with a mercury/xenon lamp (Oriel 200 W) by using a KNO_2 solution as filter. The piperidine treatments were carried out by adding piperidine (1 M, 100 μL) to the duplex solutions and by heating at 90 °C for one hour. The samples were then lyophilised and washed/lyophilised twice with water (100 μL). Fpg was provided by M. Saparbaev (Institut Gustave Roussy Villejuif-France). A typical experiment was performed by treating samples purified by gel electrophoresis with 60 ng of Fpg in 20 μL incubation buffer (Hepes/KOH 70 mM, KCl 100 mM, EDTA 1 mM, pH 7) at 37 °C for one hour. Exonuclease III was purchased from Pharmacia (200 units μL^{-1}). The enzyme (360 units) and the sample were incubated at 37 °C for 1 h in 10 μL of the enzyme buffer (HEPES/KOH 50 mM pH 7, KCl 50 mM, $CaCl_2$ 5 mM, DTT 1 mM). Samples of the various incubation mixtures (2 μL) were dissolved in 8 μL of the loading buffer (95% formamide, 0.1% xylene cyanol, 0.1% bromophenol blue). The DNA products were separated by electrophoresis on polyacrylamide gel (20% with a 19:1 ratio of acrylamide to bisacrylamide) containing urea (7 M) in TBE buffer (90 mM Tris-borate, pH 8, 2 mM EDTA). The gels were visualised by autoradiography using Kodak X-OMAT AR films and were counted with an Instant Imager (Packard Instrument).

Continuous irradiation in presence of GMP and CT-DNA: Continuous irradiation in presence of GMP or CT-DNA was performed with a mercury vapour lamp (Osram HBO 200 W) and a 2000 W quartz halogen lamp (Philips), cooled by a system of water circulation. IR (water) and UV (KNO_2) cut-off filters were inserted between the irradiation cell and the exciting source. All the experiments were performed with argon-, air- and oxygen-saturated solutions (2 mL) containing $[Ru(hat)_2phen]^{2+}$ (2.10^{-5} M) and GMP (2.10^{-3} M) or CT-DNA (expressed in phosphate equivalents).

Isolation of the photoadduct: A solution (100 mL) of $[Ru(hat)_2phen]^{2+}$ (5.6×10^{-5} M), Na_2GMP (2×10^{-3} M) and H_2GMP (10^{-3} M) (pH 6) was illuminated for 5 h in a Pyrex photoreactor, under continuous stirring and Ar bubbling, using a 125 W medium-pressure mercury lamp. The evolution of the photoreaction was followed simultaneously by absorption spectroscopy and analytical HPLC. The photoadduct was separated from the starting complex and ruthenium-containing side-products by cation-exchange chromatography. The excess of GMP was removed by HPLC, using a gradient from 0–80% acetonitrile (100–20% water) over 42 min at a flow rate of 2 mL min^{-1}. Both eluting solvents contained 0.05% trifluoroacetic acid.

Acknowledgement

The authors would like to thank Rita D'Orazio for the NMR measurements as well as Matteo Cusumano and Maria Laetizia Di Pietro (University of Messina) for the viscosity measurements. R.B. thanks the Luxembourg Ministry of Education and Vocational Training and the Action Lions Vaincre le Cancer for a Ph.D. research grant, as well as the COST D14 for financial support during a Short Term Scientific Mission. H.N. is grateful to the European T. M. R. program (ERBFMRXCT980226) for a post doc grant. The authors thank the ARC program (02/07-286) for financial support. The LEA (Laboratoire Européen Associé, Belgium-France) is also acknowledged for the fund from the Belgian FNRS (Fonds National de la Recherche Scientifique) and French CNRS (Centre National de la Recherche Scientifique).

[1] B. K. Keppler, *Metal Complexes in Cancer Chemotherapy*, Wiley-VCH, Weinheim, **1993**.

[2] A. Sigel, H. Sigel, *Metal ions in biological systems*, Marcel Decker, New York, **1996**.
[3] C. Moucheron, A. Kirsch-De Mesmaeker, J. M. Kelly in *Structure and Bonding*, *Vol. 92*, Springer, Berlin, **1998**.
[4] A. Kirsch-De Mesmaeker, J.-P. Lecomte, J. M. Kelly, *Top. Curr. Chem.* **1996**, *177*, 25–76.
[5] I. Ortmans, C. Moucheron, A. Kirsch-De Mesmaeker, *Coord. Chem. Rev.* **1998**, *168*, 233–271.
[6] M. B. Fleisher, K. C. Waterman, N. J. Turro, J. K. Barton, *Inorg. Chem.* **1986**, *25*, 3549–3551.
[7] K. E. Erkkila, D. T. Odom, J. K. Barton, *Chem. Rev.* **1999**, *99*, 2777–2795.
[8] E. Gicquel, N. Paillous, P. Vicendo, *Photochem. Photobiol.* **2000**, *72*, 583–589.
[9] C. S. Chow, J. K. Barton, *Methods Enzymol.* **1992**, *212*, 219–242.
[10] A. B. Tossi, J. M. Kelly, *Photochem. Photobiol.* **1989**, *49*, 545–556.
[11] P. Lincoln, B. Nordén, *J. Phys. Chem. B* **1998**, *102*, 9583–9594.
[12] M. Pauly, I. Kayser, M. Schmitz, M. Dicato, A. Del Guerzo, I. Kolber, C. Moucheron, A. Kirsch-De Mesmaeker, *Chem. Commun.* **2002**, 1086–1087.
[13] C. Moucheron, A. Kirsch-De Mesmaeker, J. M. Kelly, *J. Photochem. Photobiol. B* **1997**, *40*, 91–106.
[14] A. Kirsch-De Mesmaeker, C. Moucheron, N. Boutonnet, *J. Phys. Org. Chem.* **1998**, *11*, 566–576.
[15] J.-P. Lecomte, A. Kirsch-De Mesmaeker, M. M. Feeney, J. M. Kelly, *Inorg. Chem.* **1995**, *34*, 6481–6491.
[16] J.-P. Lecomte, A. Kirsch-De Mesmaeker, J. M. Kelly, A. B. Tossi, H. Görner, *Photochem. Photobiol.* **1992**, *55*, 681–689.
[17] A. Kirsch-De Mesmaeker, G. Orellana, J. K. Barton, N. J. Turro, *Photochem. Photobiol.* **1990**, *52*, 461–472.
[18] L. Jacquet, R. J. H. Davies, A. Kirsch-De Mesmaeker, J. M. Kelly, *J. Am. Chem. Soc.* **1997**, *119*, 11763–11768.
[19] L. Jacquet, J. M. Kelly, A. Kirsch-De Mesmaeker, *J. Chem. Soc. Chem. Commun.* **1995**, 913–914.
[20] M. M. Feeney, J. M. Kelly, A. B. Tossi, A. Kirsch-De Mesmaeker, J.-P. Lecomte, *J. Photochem. Photobiol. B* **1994**, *23*, 69–78.
[21] I. Haq, P. Lincoln, D. Suh, B. Nordén, B. Z. Chowdhry, J. B. Chaires, *J. Am. Chem. Soc.* **1995**, *117*, 4788–4796.
[22] A. Greguric, I. D. Greguric, T. W. Hambley, J. R. Aldrich-Wright, J. G. Collins, *J. Chem. Soc. Dalton Trans.* **2002**, 849–855.
[23] C. M. Dupureur, J. K. Barton, *Inorg. Chem.* **1997**, *36*, 33–43.
[24] Y. Jenkins, A. E. Friedman, N. J. Turro, J. K. Barton, *Biochemistry* **1992**, *31*, 10809–10816.
[25] C. Moucheron, A. Kirsch-De Mesmaeker, S. Choua, *Inorg. Chem.* **1997**, *36*, 584–592.
[26] C. Moucheron, A. Kirsch-De Mesmaeker, *J. Phys. Org. Chem.* **1998**, *11*, 577–583.
[27] J. M. Kelly, M. M. Feeney, A. B. Tossi, J.-P. Lecomte, A. Kirsch-De - Mesmaeker, *Anti-Cancer Drug Des.* **1990**, *5*, 69–75.
[28] A. Del Guerzo, A. Kirsch-De Mesmaeker, *Inorg. Chem.* **2002**, *41*, 938–945.
[29] J.-P. Lecomte, A. Kirsch-De Mesmaeker, G. Orellana, *J. Phys. Chem.* **1994**, *98*, 5382–5388.
[30] F. Pierard, A. Del Guerzo, A. Kirsch-De Mesmaeker, M. Demeunynck, J. Lhomme, *Phys. Chem. Chem. Phys.* **2001**, *3*, 2911–2920.
[31] A. Del Guerzo, *Ph. D. thesis*, Université Libre de Bruxelles, Bruxelles, **1998**.
[32] S. Satyanarayana, J. C. Dabrowiak, J. B. Chaires, *Biochemistry* **1992**, *31*, 9319–9324.
[33] G. Cohen, H. Eisenberg, *Biopolymers* **1966**, *4*, 429–440.
[34] M. Cusumano, M. L. Di Pietro, A. Giannetto, *Inorg. Chem.* **1999**, *38*, 1754–1758.
[35] M. Cusumano, M. L. Di Pietro, A. Giannetto, F. Nicolò, E. Rotondo, *Inorg. Chem.* **1998**, *37*, 563–568.
[36] M. Cusumano, M. L. Di Pietro, A. Giannetto, *Chem. Commun.* **1996**, 2527–2528.
[37] M. Howe-Grant, S. J. Lippard, *Biochemistry* **1979**, *18*, 5762–5769.
[38] P. Vicendo, S. Mouysset, N. Paillous, *Photochem. Photobiol.* **1997**, *65*, 647–655.
[39] B. Armitage, *Chem. Rev.* **1998**, *98*, 1171–1200.
[40] C. J. Burrows, J. G. Muller, *Chem. Rev.* **1998**, *98*, 1109–1151.
[41] D. Angelov, A. Spassky, M. Berger, J. Cadet, *J. Am. Chem. Soc.* **1997**, *119*, 11373–11380.
[42] S. Boiteux, E. Gajewski, J. Laval, M. Dizdaroglu, *Biochemistry* **1992**, *31*, 106–110.
[43] V. Duarte, D. Gasparutto, M. Jaquinod, J. Cadet, *Nucleic Acids Res.* **2000**, *28*, 1555–1563.
[44] L. Gros, M. K. Saparbaev, J. Laval, *Oncogene* **2002**, *21*, 8905–8925.
[45] A.-L. Lu, X. Li, Y. Gu, P. M. Wright, D.-Y. Chang, *Cell Biochem. Biophys.* **2001**, *35*, 1–30.
[46] J. Cadet, T. Douki, S. Frelon, S. Sauvaigo, J.-P. Pouget, J.-L. Ravanat, *Free Radical Biol. Med.* **2002**, *33*, 441–449.
[47] M. Gniazdowski, C. Cera, *Chem. Rev.* **1996**, *96*, 619–634.
[48] J. Reynisson, S. Steenken, *Phys. Chem. Chem. Phys.* **2002**, *4*, 527–532.
[49] J. Reynisson, S. Steenken, *Phys. Chem. Chem. Phys.* **2002**, *4*, 5346–5352.
[50] S. C. Weatherly, I. V. Yang, H. H. Thorp, *J. Am. Chem. Soc.* **2001**, *123*, 1236–1237.
[51] J.-L. Ravanat, T. Douki, J. Cadet, *J. Photochem. Photobiol. B* **2001**, *63*, 88–102.
[52] S. Steenken, *Chem. Rev.* **1989**, *89*, 503–520.
[53] E. O. Hole, W. H. Nelson, D. M. Close, E. Sagstuen, *J. Chem. Phys.* **1987**, *86*, 5218–5219.
[54] L. P. Candeias, S. Steenken, *J. Am. Chem. Soc.* **1989**, *111*, 1094–1099.
[55] S. Steenken, S. V. Jovanovic, *J. Am. Chem. Soc.* **1997**, *119*, 617–618.
[56] L. Tan-Sien-Hee, L. Jacquet, A. Kirsch-De Mesmaeker, *J. Photochem. Photobiol. A* **1994**, *81*, 169–176.
[57] Q. G. Mulazzani, H. Sun, M. Z. Hoffman, W. E. Ford, M. A. J. Rodgers, *J. Phys. Chem.* **1994**, *98*, 1145–1150.
[58] C. J. Timpson, C. C. Carter, J. Olmsted, *J. Phys. Chem.* **1989**, *93*, 4116–4120.
[59] N. Paillous, P. Vicendo, *J. Photochem. Photobiol. B* **1993**, *20*, 203–209.
[60] C. Sheu, C. S. Foote, *J. Am. Chem. Soc.* **1993**, *115*, 10446–10447.
[61] C. Sheu, C. S. Foote, *J. Am. Chem. Soc.* **1995**, *117*, 6439–6442.
[62] L. Torun, H. Morrison, *Photochem. Photobiol.* **2003**, *77*, 370–375.
[63] A. P. Breen, J. A. Murphy, *Free Radical Biol. Med.* **1995**, *18*, 1033–1077.
[64] S. Raoul, M. Berger, G. W. Buchko, P. C. Joshi, B. Morin, M. Weinfeld, J. Cadet, *J. Chem. Soc. Perkin Trans. 2* **1996**, *3*, 371–381.
[65] J. M. Kelly, D. J. McConnell, C. OhUigin, A. B. Tossi, A. Kirsch-De - Mesmaeker, A. Masschelein, J. Nasielski, *J. Chem. Soc. Chem. Commun.* **1987**, 1821–1823.
[66] J. D. McGhee, P. H. von Hippel, *J. Mol. Biol.* **1974**, *86*, 469–489.
[67] G. Scatchard, *Ann. N. Y. Acad. Sci.* **1949**, *51*, 660–672.
[68] M. T. Record, T. M. Lohman, P. de Haseth, *J. Mol. Biol.* **1976**, *107*, 145–158.
[69] M. T. Record, C. F. Anderson, T. M. Lohman, *Q. Rev. Biophys.* **1978**, *11*, 103–178.

Received: June 10, 2004
Published online: January 24, 2005

